Clim Dyn (2011) 36:1649–1658
DOI 10.1007/s00382-011-1067-4

# On tropospheric adjustment to forcing and climate feedbacks

**R. A. Colman · B. J. McAvaney**

Received: 1 December 2008 / Accepted: 25 May 2009 / Published online: 5 April 2011


**Abstract** Motivated by findings that major components of so-called cloud 'feedbacks' are best understood as rapid responses to $CO_2$ forcing (Gregory and Webb in J Clim 21:58–71, 2008), the top of atmosphere (TOA) radiative effects from forcing, and the subsequent responses to global surface temperature changes from all 'atmospheric feedbacks' (water vapour, lapse rate, surface albedo, 'surface temperature' and cloud) are examined in detail in a General Circulation Model. Two approaches are used: applying regressions to experiments as they approach equilibrium, and equilibrium experiments forced separately by $CO_2$ and patterned sea surface temperature perturbations alone. Results are analysed using the partial radiative perturbation ('PRP') technique. In common with Gregory and Webb (J Clim 21:58–71, 2008) a strong positive addition to 'forcing' is found in the short wave (SW) from clouds. There is little evidence, however, of significant global scale rapid responses from long wave (LW) cloud, nor from surface albedo, SW water vapour or 'surface temperature'. These responses may be well understood to first order as classical 'feedbacks'—i.e. as a function of global mean temperature alone and linearly related to it. Linear regression provides some evidence of a small rapid negative response in the LW from water vapour, related largely to decreased relative humidity (RH), but the response here, too, is dwarfed by subsequent response to warming. The large rapid SW cloud response is related to cloud fraction changes—and not optical properties—resulting from small cloud decreases ranging from the tropical mid troposphere to the mid latitude lower troposphere, in turn associated with decreased lower tropospheric RH. These regions correspond with levels of enhanced heating rates and increased temperatures from the $CO_2$ increase. The pattern of SW cloud fraction response to SST changes differs quite markedly to this, with large positive radiation responses originating in the upper troposphere, positive contributions in the lowest levels and patterns of positive/negative contributions in mid latitude low levels. Overall SW cloud *feedback* was diagnosed as negative, due to the substantial negative SW feedback in cloud optical properties more than offsetting these. This study therefore suggests the rapid response to $CO_2$ forcing is (apart from a possible small negative response from LW water vapour) essentially confined to cloud fraction changes affecting SW radiation, and further that significant feedbacks with temperature occur in all cloud components (including this one), and indeed in all other classically understood 'feedbacks'.

R. A. Colman (✉) · B. J. McAvaney
Centre for Australian Weather and Climate Research,
Bureau of Meteorology, GPO Box 1289, Melbourne,
VIC 3001, Australia
e-mail: r.colman@bom.gov.au

## 1 Introduction

The range of climate sensitivity between different General Circulation Models (GCMs) remains large (Randall et al. 2007). Climate feedbacks and particularly cloud feedbacks remain a major source of this uncertainty (Randall et al. 2007; Webb et al. 2006; Bony et al. 2006). A recent study by Gregory and Webb (2008) following on earlier work by Gregory et al. (2004) has provided important new insight into the response of clouds to forced climate change. They found that rapid tropospheric adjustment to $CO_2$ forcing induced a change in global top of atmosphere (TOA) 'cloud radiative forcing' (CRF) across a range of models. They further found that in most cases there was little

change in CRF in response to subsequent warming. As a result, they argue that much of the cloud response in these models should be classified primarily as part of the forcing rather than a climate feedback.

These findings are important for a number of reasons. They challenge the concept of cloud feedback as a response mediated by global scale warming, a point forcefully made by Stephens (2005), who argued that there is a lack of theoretical or empirical evidence to link cloud responses to global time-mean changes in surface temperature. If cloud changes are primarily a rapid response to forcing alone, we would expect them to occur contemporaneously with the forcing, rather than delayed by the thermal inertia of the climate system. If sensitivity to temperature is expected to be intrinsically small it would also affect possible strategies for metrics related to reliability of cloud feedback resulting from interannual variability (e.g. Bony and Dufresne 2005). In particular it would imply that temperature based analogues have very limited applicability for assessing cloud response under externally forced climate change. It also has strong implications for the most appropriate definition of forcing (Gregory and Webb 2008), and for the calculation of a measure which can provide a most robust estimate of climate response to a range of different forcing (as discussed at length by Hansen et al. 2002, 2005 and Shine et al. 2003), which has implications for the projection of climate change using simple models. Finally, an investigation using the CRF approach by Andrews and Forster (2008) found evidence of rapid adjustments to the 'clear sky' response in some models (suggesting possible impacts from changes to water vapour, lapse rate and surface albedo) and a rapid net 'clear sky' response was diagnosed under solar forcing by Lambert and Faull (2007) in the Hadley Centre GCM.

Important questions remain however, particularly in understanding the differing processes operating at the different timescales. In particular what is the nature of the rapid cloud response to $CO_2$ forcing, and which parts, if any, of it are sensitive to the following warming? Furthermore do significant rapid adjustments form part of other traditionally understood 'feedbacks', such as those due to water vapour or lapse rate, which might thereby contribute to the rapid response? Are the results—particularly in the long wave (LW)—affected by the use of 'cloud radiative forcing' to assess cloud change impacts on radiation? To address such questions this short note uses the 'partial radiative perturbation' (PRP) technique (see below) of analysing TOA radiative changes, looking at a single model in detail. This method permits structural features of the radiative response to be diagnosed, and removes ambiguities present from the use of CRF changes, since the latter does not cleanly separate the radiative response due to cloud changes from the cloud masking of TOA clear sky fluxes, and cannot separately evaluate water vapour, lapse rate and surface temperature impacts (Colman 2003; Soden et al. 2004).

The second part of this paper briefly describes the model and experiments, and the PRP technique. The third section discusses the results for TOA radiation analysis, separating the impacts of rapid, forcing-sensitive tropospheric adjustments from those of longer term temperature driven feedbacks, and comparing with experiments in which $CO_2$ and sea surface temperature (SST) changes are separately applied. The final section contains concluding remarks.

## 2 Experiments and quantification of radiative perturbations

### 2.1 Model and experiments

The model used here is a version of the Australian Bureau of Meteorology Research Centre (BMRC) now Centre for Australian Weather and Climate Research (CAWCR) atmospheric General Circulation Model (GCM) coupled to a 50 m deep mixed layer ocean and a thermodynamic sea ice model. Horizontal resolution is triangular wave 47, with 17 levels in the vertical. It is described in Colman et al. (2001) although there are some changes to the prognostic cloud scheme, permitting mixed phase clouds (Rotstayn 1997; Rotstayn et al. 2000), as well as specifying modified LW and short wave (SW) optical properties (adopting those of Chou et al. 1998; Sun and Pethick 2002, respectively), with the radiation parametrisation updated to the Sun Edward Slingo scheme (Sun and Rikus 1999). Control experiments specified $CO_2$ levels at 375 parts per million (ppm), with $CO_2$ then instantaneously doubled (an ensemble of two) or quadrupled, with the model then run to equilibrium, then for a further 10–20 years. Further experiments were performed with sea surface temperatures (SSTs) prescribed from the equilibriated portion of the $1 \times CO_2$ and $4 \times CO_2$ experiments, with $CO_2$ levels specified at 375 and 1,380 ppm (described below).

### 2.2 Partial radiative perturbation analysis

For a small climate perturbation (say a change in $CO_2$ concentration) the change to TOA radiation, $R$, at a given location in the model can be written (where the tilde '$\sim$' denotes the vertical profile of a variable):

$$\delta R \approx \delta R_{\tilde{T}*} + \delta R_{\tilde{\Gamma}} + \delta R_{\tilde{q}} + \delta R_{\tilde{C}} + \delta R_{a} + \delta R_{C\tilde{O}_2} \qquad (1)$$

where $T*$ is the surface temperature change applied uniformly throughout the atmosphere, $\Gamma$ the lapse rate, $q$ the specific humidity, $C$ the cloud distribution and $a$ the surface albedo. These radiative perturbations are determined

in this study by offline running of the radiation code on instantaneous, daily, archives of model fields, using the so-called "Partial Radiative Perturbation" technique (e.g. Wetherald and Manabe 1988). Details of the calculations are given in Colman et al. (2001).

To better understand the cloud changes, the cloud radiative response is divided into separate components due to fraction (i.e. the 3D cloud distribution), $C_F$, and optical property changes $C_O$, viz:

$$\delta R_{\tilde{C}} \approx \delta R_{\tilde{C}_F} + \delta R_{\tilde{C}_O}. \quad (2)$$

## 3 Results and discussion

Figure 1 shows the global mean TOA LW and SW radiation changes, calculated using PRP, as a function of global mean temperature for the different 'feedback' components listed in Eq. 1 (i.e. occurring after instantaneous doubling or quadrupling of $CO_2$, as the model adjusts towards equilibrium). Shown separately are results for the double and quadruple $CO_2$ forcing experiments (quadrupled $CO_2$ radiation values having been scaled down by a factor of two for ease of comparison with the other cases). Note that the equilibrium mean surface temperature change is relatively small in this model, at around 2.4 K. The gradient of these responses can be understood as the temperature related 'feedback', and the intercept the 'rapid' response from atmospheric adjustment (Gregory et al. 2004). Gradients and intercepts are shown in (the right hand columns of) Table 1.

### 3.1 Water vapour, lapse rate and surface albedo responses

Figure 1 shows that the water vapour (both LW and SW), lapse rate, surface albedo and LW cloud radiative perturbations all vary close to linearly with temperature, with small or zero rapid adjustments, and so that they indeed behave to a good approximation as classically understood "global feedbacks". The only statistically significant exception is the small initial adjustment impacts for LW water vapour, with an extrapolated response of $-0.30 \pm 0.23$ W m$^{-2}$ (range indicating 95% confidence) indicating it is just significantly different from zero at the 5% level.

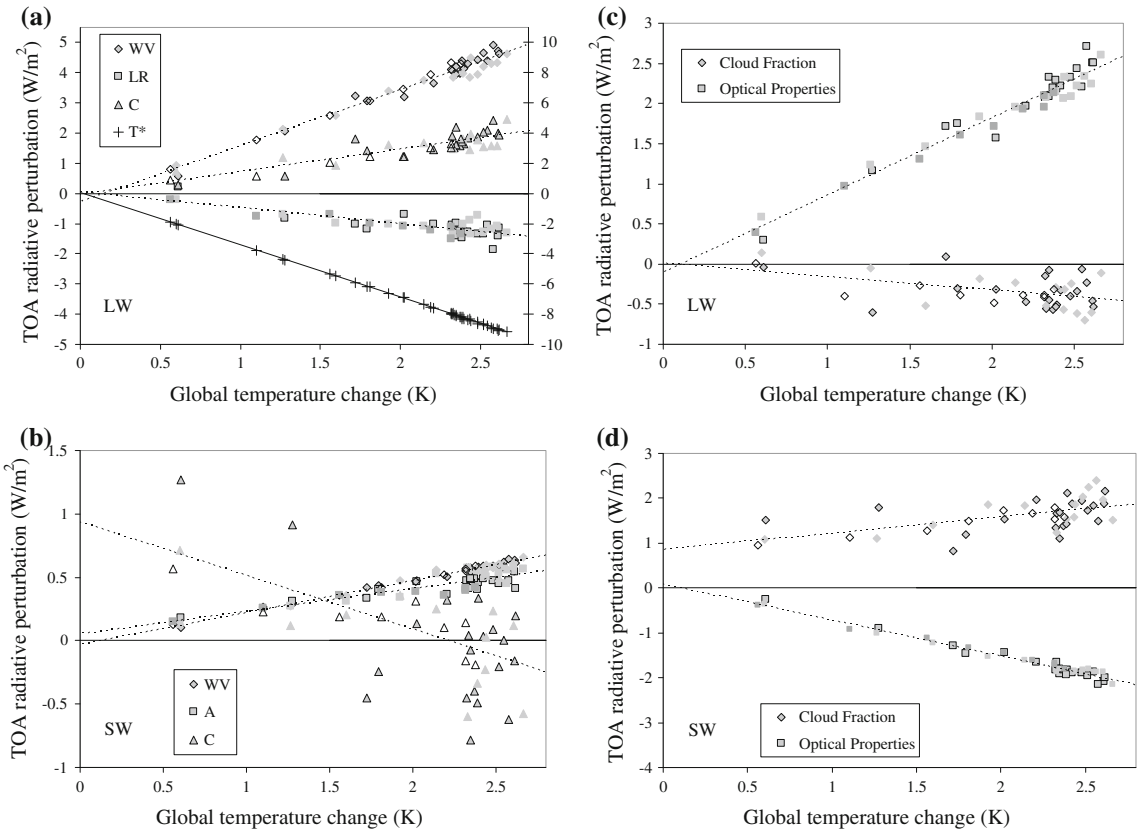


**Fig. 1** Evolution with temperature of TOA global radiation perturbations (W m$^{-2}$) for **a** LW water vapour (*WV*), lapse rate (*LR*), clouds (*C*) and 'surface temperature' (*T**), **b** SW water vapour, surface albedo (*A*) and cloud terms. Also shown are cloud component changes for cloud fraction, $C_F$, and cloud optical properties, $C_O$, for **c** LW and **d** SW. Individual climate change experiments are shown as follows: 2 × $CO_2$: *gray* and *light gray symbols*, (scaled) 4 × $CO_2$: *gray with dark border symbols*. *Dotted lines* are lines of best fit, encompassing all experiments. The surface temperature term in **a** refers to the right-hand axis

**Table 1** Top of atmosphere global radiative perturbations (W $m^{-2}$) for a range of parameters (refer Eqs. 1 and 2): $T^*$ is the surface temperature change applied uniformly throughout the atmosphere, $\Gamma$ the lapse rate, $q$ the specific humidity, $a$ the surface albedo, and $C_F$, and $C_O$ the cloud fraction and optical property changes respectively

| | $CO_2$ (W $m^{-2}$) | SST | $CO_2$ &SST | 4 × $CO_2$ (free) | Intercept (W $m^{-2}$) | Slope (W $m^{-2}$ $K^{-1}$) |
|---|---|---|---|---|---|---|
| SW | | | | | | |
| $a$ | 0.05 | 0.55 | 0.55 | 0.41 | 0.05 ± 0.06 | 0.18 ± 0.03 |
| $C_F$ | 0.80 | 1.3 | 2.0 | 1.9 | 0.85 ± 0.36 | 0.36 ± 0.17 |
| $C_O$ | −0.05 | −1.7 | −1.7 | −1.8 | 0.09 ± 0.10 | −0.80 ± 0.05 |
| LW | | | | | | |
| $T^*$ | −0.60 | −8.5 | −9.0 | −9.0 | 0.06 ± 0.05 | −3.47 ± 0.02 |
| $q$ | 0.05 | 4.6 | 4.6 | 4.8 | −0.30 ± 0.23 | 1.87 ± 0.10 |
| $\Gamma$ | 0.0 | −1.3 | −1.3 | −1.5 | 0.05 ± 0.27 | −0.52 ± 0.12 |
| $C_F$ | 0.0 | −0.55 | −0.55 | −0.50 | 0.01 ± 0.22 | −0.16 ± 0.10 |
| $C_O$ | 0.0 | 2.2 | 2.2 | 2.3 | −0.11 ± 0.15 | 0.96 ± 0.07 |
| $\Delta T_s$ (K) | 0.17 | 2.35 | 2.52 | 2.59 | | |

Experiments shown are with $CO_2$ quadrupled, with SSTs fixed ('$CO_2$'); SST changes specified with fixed $CO_2$ ('SST'), both SST and $CO_2$ changes specified ('$CO_2$&SST') and the original unconstrained 4 × $CO_2$ experiment ('4 × $CO_2$ (free)'). All experiments are run to equilibrium. Positive numbers indicate increased radiation downwards (i.e. positive forcing/feedback), and values have been scaled by 0.5 for comparison with 2 × $CO_2$ experiments. Refer to text for method of calculation of radiative perturbations. $\Delta T_s$ shows the change in global surface temperature (in K) for each experiment. The right two columns show the 'Intercept' (W $m^{-2}$) and 'slope' (W $m^{-2}$ $K^{-1}$) from the regression fits shown in Fig. 1 (with ranges indicating 95% confidence limits)

This was further examined, dividing the term into that component implied by constant relative humidity (RH)—i.e. where changes are determined by air temperature changes alone—and from changes in RH. Colman (2004) gives a full description of this division. These components were also further stratified into land/sea-ice and ocean changes. The only statistically significant contribution was found to be at the global scale (all surface types), with a contribution of −0.15 ± 0.12 W $m^{-2}$ from RH changes, indicating that some or all of the response can be explained by a small, rapid decrease in RH. Indeed examination of a time series of vertical RH profile reveals a small reduction in the mid to lower troposphere, appearing rapidly following $CO_2$ doubling (not shown). Consistent with this, Andrews and Forster (2008) found a small rapid reduction in atmospheric water content across seven 'slab ocean' models examined from the CMIP3 (Coupled Model Intercomparison Project, Phase 3) model ensemble. Also consistent with this is the pattern of RH changes found in experiments in which $CO_2$ is instantaneously increased, with SSTs held fixed (see Fig. 3 below and related discussion).

There is also a suggestion of a very small (0.05 ± 0.06 W $m^{-2}$) positive rapid surface albedo response, although it is not statistically significant at the 5% level. Note that by comparison Andrews and Forster (2008) found a small SW clear sky response in some of the CMIP3 models, with most being negative.

In summary, for water vapour, lapse rate and surface albedo, any 'rapid' response is dwarfed by their much larger response to global temperature change, so for the most part these should still be thought of as classical 'feedbacks'.

### 3.2 Cloud responses

Short wave effects of cloud behave very differently from all other factors, with an extrapolated rapid response to $CO_2$ forcing of around 1 W $m^{-2}$ (0.94 ± 0.43 W $m^{-2}$) subsiding with global warming (at a rate of −0.42 ± 0.20 W $m^{-2}$ $K^{-1}$) to be close to zero at equilibrium. The variation with temperature may be considered the true cloud SW 'feedback' of the model. Without considering the rapid response, it is apparent that a 'feedback' term of close to zero would have been diagnosed. Dividing cloud responses into those due to cloud fraction and optical property changes (Fig. 1c, d), reveals a close to linear temperature dependence of optical property changes in both LW and SW, with no suggested rapid response. These in turn are found to be the sum of quasi-linear radiation changes originating from increasing cloud water content, and decreased fraction of frozen water within clouds (not shown), which as expected are sensitive functions of large scale temperature changes. The rapid SW cloud response is therefore from cloud fraction changes alone. The nature of these changes is examined further below.

These values may be compared with the SW cloud rapid responses listed by Gregory and Webb (2008) and Andrews and Forster (2008) of 0.49 ± 0.41 and 0.65 ± 0.44 W $m^{-2}$ respectively for two different ensembles of 'slab ocean'

GCMs (where the range denotes 1 standard deviation across the models). Although the results from these two papers used the "CRF" method, rather than PRP, they may be directly compared with the present, since results here suggest the rapid response from other variables which affect the SW (water vapour and surface albedo) is small, and the SW 'clear sky' rapid response found by both these studies is small. The comparison indicates that the present SW cloud rapid response is consistent with those studies, although lying towards the high end of the model range.

Despite the LW cloud term showing little or no initial global mean response to the forcing, if LW CRF is plotted against temperature, it implies an extrapolated zero value of around $-0.5$ W m$^{-2}$ (not shown). The present analysis suggests that the bulk of this value does not represent a rapid cloud response, nor a cloud 'masking' of water vapour, lapse rate or 'surface temperature' feedbacks, as these are shown to be small in response to the initial forcing. Indeed only the LW water vapour 'rapid response' term is distinguishable from zero, and there the presence of clouds provides a small positive masking effect—reducing the best estimate of the 'clear sky' value from $-0.5$ to $-0.3$ W m$^{-2}$: a change of $+0.2$ W m$^{-2}$.

Analysing the cloud *masking* of $CO_2$ forcing (by performing forcing calculations with and without instantaneously zero clouds), shows they have an impact of around $-0.6$ W m$^{-2}$, enough to explain the CRF discrepancy from zero. Note that this masking value is roughly a factor of three greater than the (erroneous) earlier calculation of Colman (2003), quoted by Gregory and Webb (2008), and is consistent with the value obtained by Soden et al. (2008). This masking occurs because instantaneously increasing $CO_2$ reduces TOA upward radiation from the atmosphere, but does not effect emission from clouds, so instantaneous 'all-sky' changes in TOA radiation are smaller than would be the case for a (hypothetical) clear sky planet (Gregory and Webb 2008). Removing the $CO_2$ masking from the range for rapid LW CRF change of $-0.85 \pm 0.21$ W m$^{-2}$ found by Gregory and Webb (2008), suggests a small negative change in CMIP3 models (consistent with the range $-0.23 \pm 0.10$ W m$^{-2}$ found by Andrews and Forster (2008), who did explicitly allow for the masking). The current findings are slightly more positive than those of these two ensembles, which may indicate either a differing cloud response in the LW, or a rapid response to water vapour or lapse rate in CMIP3 models in those studies, which as a consequence impacts on LW CRF.

### 3.3 Comparison with fixed SST experiments

What is the nature of the rapid SW cloud response to forcing compared with the response to increasing temperatures? To investigate this, a further three experiments were run. In the first, SSTs were held fixed at 'control' values, but $CO_2$ quadrupled. The approach used here follows that of Hansen et al. (2002), permitting land and sea-ice temperatures to change. This avoids the complexity of fixing these temperatures (as in the method of Shine et al. 2003), but does have the result that they increase by approximately 1 K, giving a global temperature increase of 0.4 K. In the second experiment, SST and sea-ice changes derived from the equilibrium $4 \times CO_2$ experiment were applied to the model, but $CO_2$ levels maintained at control values. Mean surface temperature change was 4.7 K. In the third, both increased SSTs and $CO_2$ levels were applied, for a temperature change of 5.0 K (within 0.3% of the sum of the previous two). This latter experiment provides a check with the results of the 'freewheeling' mixed layer ocean $4 \times CO_2$ experiment (which provides a warming also of 5.0 K), as well as checking the 'linearity' of the separate SST and $CO_2$ forced experiments.

Global changes in TOA radiation from terms in Eqs. 1 and 2 are given in Table 1 (scaled by a factor of 0.5 to enable comparison with earlier $2 \times CO_2$ results). The radiative perturbations for the combined SSTs and $CO_2$ change are generally a close approximation of the sum of the separate changes (all within 0.1 W m$^{-2}$ or better than 10%), and in turn with the 'freewheeling'$4 \times CO_2$ experiment (to within 0.15 W m$^{-2}$). Note that the there are some relatively greater differences when considered over particular surface types, and in particular over land, where the SW $C_F$ response disagrees by 0.5 W m$^{-2}$.

For the $CO_2$ forcing alone all net global response terms are small, apart from surface temperature ($-0.6$ W m$^{-2}$) and the SW $C_F$ terms (0.8 W m$^{-2}$). The latter is statistically consistent with the results from regression above. Furthermore global LW/SW $C_O$ terms and LW $C_F$ are close to zero consistent with the results from linear fits in Fig. 1. The non-zero surface temperature term arises from the (scaled) roughly 0.5 K warming over land and sea-ice (which are not held fixed). This result is different from that implied by the linear fit to 'rise time' (i.e. pre-equilibration) warming, which is close to zero (Fig. 1a). It is, however, small (<10%) compared with the final absolute value from the SST changes. Finally note that the small (0.05 W m$^{-2}$) positive albedo response is consistent in magnitude with that implied by the regression approach above—although the latter was found to be not statistically different from zero at the 5% level.

It should be noted, of course, that while these two approaches (the radiation perturbation regression and the fixed SST method) are to a large extent measuring the same thing they are not in fact the same, and so do not necessarily give the same results (Gregory and Webb 2008). For example the regression technique sets no constraints on local temperature changes, requiring only that global mean

temperature change be zero. The fixed-SST experiments however constrain SST everywhere, so most of the globe has local (surface) temperature change equal to zero. At the same time it allows the land surface and sea-ice to warm, so it is unsurprising, for example, to find a diagnosed albedo response.

### 3.4 Vertical profile of responses

The vertical and meridional distribution of contributions to TOA SW and LW $C_F$ radiative responses are shown in Fig. 2 for the '$CO_2$' and 'SST' experiments. These figures represent the location of contributions to the TOA radiative response due to cloud fraction changes (i.e. with optical properties held unchanged). An obvious difference is that the SST 'forced' experiments contain large contributions from the upper troposphere, which are weak or absent from the $CO_2$ forcing alone. For the LW, since the contributions must originate mostly from this region (because of the temperature contrast with the surface), the rapid global $C_F$ response is weak.

For the SW, again, upper tropospheric contributions are weak under $CO_2$ forcing alone (Fig. 2a), however there are now significant positive contributions from an arc extending from the surface in mid-latitudes to around 600 hPa in the tropics. Figure 2a also shows there to be weak negative contributions from SW $C_F$ in the tropics and sub-tropics at the very lowest levels (below 900 hPa), which are associated with small increases in low cloud (around 0.5%) in the global mean.

The patterns differ considerably for the SST change forced experiments (Fig. 2c, d). In these experiments upper tropospheric decreases in high cloud produce significant positive contributions to SW $C_F$ "feedback", absent from the $CO_2$ forcing alone. Strong positive contributions from *decreased* very low-level cloud are also seen equatorward of around 50° (dominated by oceanic changes). At higher latitudes low-level negative contributions are seen, particularly strong in the southern hemisphere. These are associated with a poleward migration of the storm tracks—an effect absent under the $CO_2$ forcing alone. Substantial and widespread positive areas are also seen throughout the bulk of the troposphere, associated with broadscale decreases in cloud amount at most levels outside the polar regions (not shown).

The differences in vertical profiles, then, of the cloud "feedbacks" (or rather cloud change induced radiative response) is striking between the SST and $CO_2$ induced

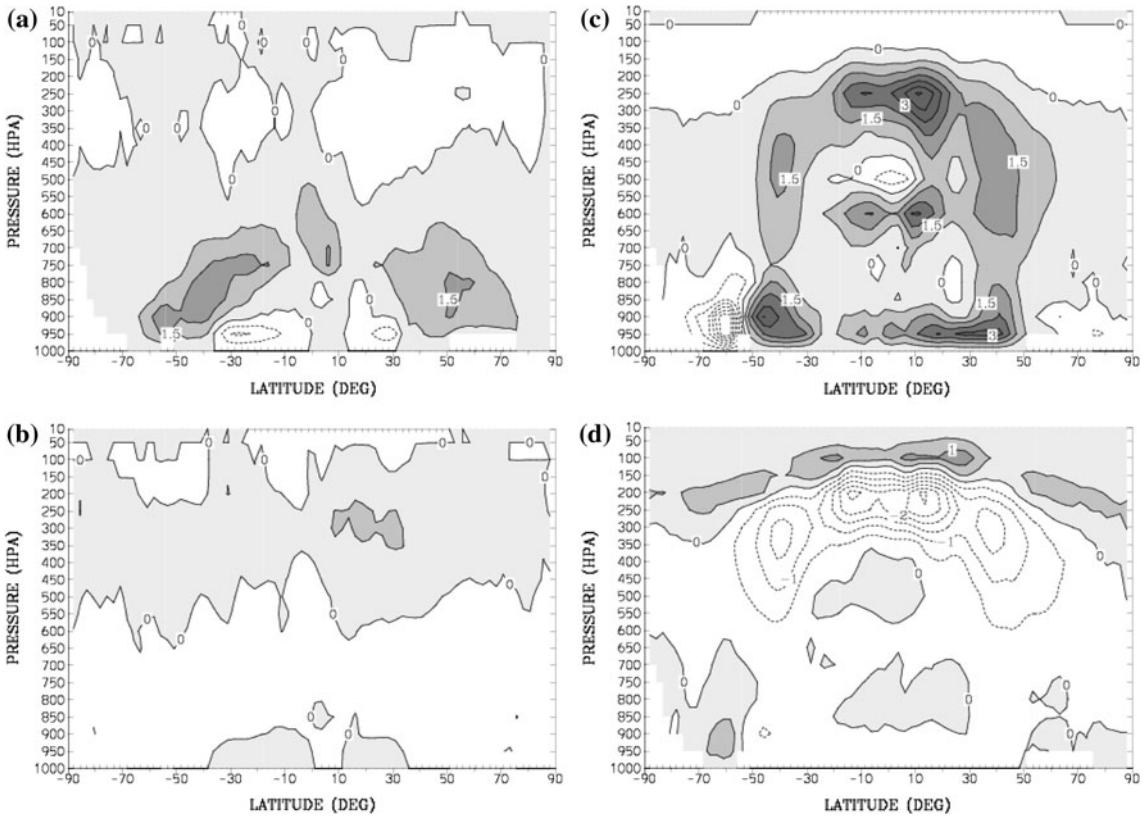


**Fig. 2** Zonally averaged contributions to TOA radiative perturbations for cloud fraction changes, $C_F$ (expressed in W m$^{-2}$ per 100 hPa layer) for **a** SW and **b** LW for $CO_2$ quadrupled (with SSTs held fixed) and **c** SW and **d** LW for SST changes specified (with $CO_2$ held fixed). Contour intervals are: **a**, **c** 0.75 W m$^{-2}$ (100 hPa)$^{-1}$, **b**, **d** 0.5 W m$^{-2}$ (100 hPa)$^{-1}$

changes. What is the source of these differences? Cloud fraction in the model is diagnosed from RH (Rotstayn 1997), and global profiles of changes in temperature and RH are summarised in Fig. 3. Firstly, it is notable that although the magnitude of the warming in the two cases is so different, RH change *magnitudes* are similar (although at quite different levels). There is a maximum in the global warming profile under $CO_2$ forcing alone at around 700–800 hPa, with a simultaneous globally averaged decrease in RH (approximately 2%) and cloud amount (approximately 1%) around these levels. This change is also qualitatively consistent with the a linear fit to $2 \times CO_2$ 'rise time' results (not shown) which indicate an initial rapid decrease in global mean RH in the mid to lower troposphere and a decrease in mid level cloud of roughly 1% (which is then followed by gradual recovery as SSTs increase).

What processes lead to the rapid lower tropospheric decrease in RH and cloud amount after $CO_2$ quadrupling? This complex question is beyond the scope of the present paper; however there is a suggestive similarity between the meridional pattern of instantaneous heating rate changes following the $CO_2$ quadrupling, shown in Fig. 4a, and the consequent SW $C_A$ radiative perturbations (Fig. 2a). Of course the two are not directly connected: cloud amount in the model is a function solely of RH (Rotstayn 1997), which has tendencies depending on changes to both temperature and specific humidity; in turn likely to be dependent upon changes to vertical stability and circulation. Temperature and RH change patterns (Fig. 4b, c) indeed show gross similarities to that of the heating rates ('arcs' of maximum warming/cooling corresponding to the maximum warming/cooling tendencies), however there are also important pattern differences, particularly at high latitudes and the equator. Note that the overall 'mirroring' between the two lower atmospheric 'arcs' (also apparent in the vertical global profiles shown in Fig. 3) is accounted for by calculations which show that the change in RH implied by the atmospheric temperature increase alone accounts for around 2/3 of the RH change maxima at 800 hPa throughout the sub-tropics, and all of it poleward of 40°: i.e. temperature rather than specific humidity changes are most important for much of the rapid lower tropospheric RH (and therefore SW cloud radiation) response seen in this model.

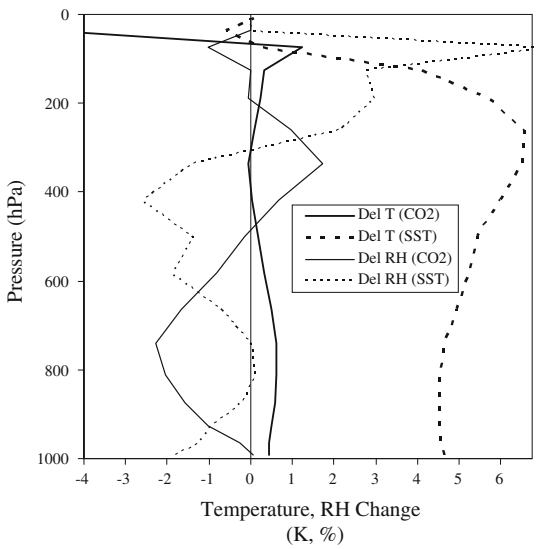


**Fig. 3** Global mean vertical changes in temperature and RH for experiments in which $CO_2$ is instantaneously quadrupled with SSTs fixed (*solid lines*) and SST increased with $CO_2$ held fixed (*dashed lines*)

### 3.5 Land/sea contrasts

A final note on comparisons between the two techniques for analysing rapid adjustment radiation responses is that other substantial separate land/sea-ice and ocean responses occur in the $CO_2$ alone forcing experiment, not apparent from the global numbers in Table 1. The small global lapse rate radiative response disguises surprisingly large offsetting responses: of $-0.6$ and 1.2 W m$^{-2}$ over ocean and land/sea-ice respectively. There is a global increase in lapse rate over land/sea-ice of approximately 0.5 K between the surface and 250 hPa, comparable to that induced by SST increases, although with a somewhat different profile (the latter showing a minimum at around 300 hPa, with large cooling above—not shown). Over ocean, on the other hand, greatest relative warming occurs at around 750 hPa for the $CO_2$ induced changes (consistent with Fig. 4), but at around 300 hPa, and more than a factor of five larger for the SST induced changes, consistent with the much larger lapse rate radiative response in the latter. The global LW $C_F$ patterns shown in Fig. 2 are dominated by ocean contributions. When the land/sea-ice alone are considered, there is evidence of some $CO_2$ forcing induced upper tropospheric cloud contribution in the LW, which make a small positive contribution, opposite in the sign to that over land/sea-ice when forced by SSTs (not shown).

Finally, radiation responses from water vapour responses to $CO_2$ alone are $-0.05$ W m$^{-2}$ over the ocean (statistically consistent, but smaller than the value obtained from the regression method above), but are stronger and positive (0.3 W m$^{-2}$) over land/sea-ice. Given the large land response with the findings above, the fixed SST experiments produce a small positive water vapour response globally, and the source of the small implied negative water vapour term found by regression above remains unclear in these experiments. The performance of fixed land/sea-ice temperature experiments (although technically difficult to perform with a GCM) may be required to resolve this question.

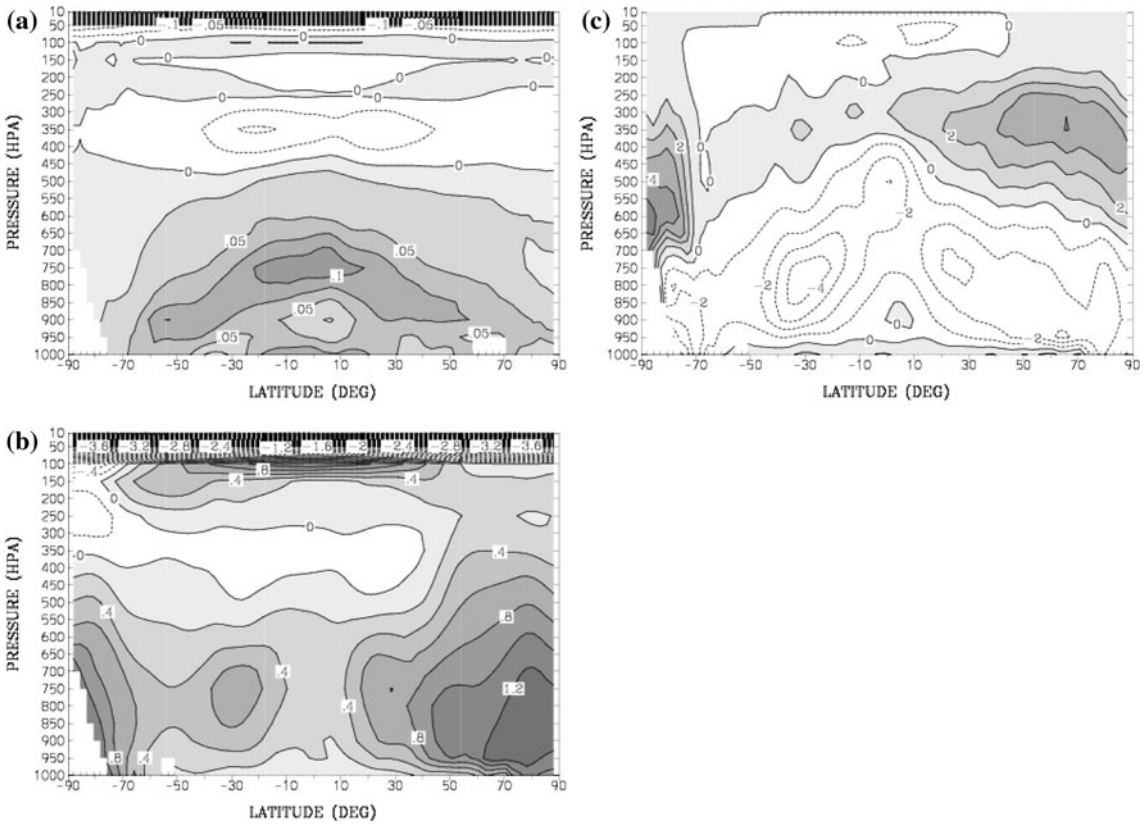


**Fig. 4** **a** Zonal mean LW radiative heating rate (K/day) from a quadrupling of $CO_2$ (but with SSTs unchanged). **b**, **c** equilibrium changes in temperature (K) and RH (%). All values shown represent means over the annual cycle

Note however that both experiments imply that any global rapid response from water vapour is small compared to its subsequent temperature related response.

## 4 Summary and conclusions

This short note has examined the rapid responses to forcing, and the subsequent responses to global surface temperature changes from changes to water vapour lapse rate, surface albedo, 'surface temperature' and cloud in a GCM—processes normally associated with global scale "feedbacks". Two approaches have been used: applying regressions to $CO_2$ forced experiments as they approach equilibrium (following Gregory and Webb 2008), and equilibrium experiments forced by $CO_2$ (alone), SST perturbations (alone) and both (qflux adjusted ocean; e.g. Hansen et al. 2005; Gregory and Webb 2008), and the results analysed using the partial radiative perturbation ('PRP') technique.

At a global scale, statistical consistency was found between the methods for the magnitude of the "rapid response" to $CO_2$ forcing, except for the surface temperature and the LW water vapour terms. There is little evidence of substantial global scale rapid responses from SW water vapour, cloud optical properties (SW/LW) or from cloud fraction changes in the LW. There is the suggestion of a very small rapid surface albedo response, although this was not clearly statistically significant. The responses to temperature of all these variables are close to linear, so they can be well understood to a close approximation as classical 'feedbacks' in this model. Linear regression suggests a small but (just) significant rapid negative response from water vapour to $CO_2$ forcing, related in part at least to decreased RH. Although decreased RH in lower layers is seen in the set of experiments with $CO_2$ increased and SSTs held fixed, there are contrasting increases aloft, in the region to which water vapour radiative response is most sensitive (Held and Soden 2000). The small net (positive) impact on TOA radiation results from contrasting negative/positive response over ocean/land. Experiments with fixed land temperatures would be necessary to unravel these (small) differences.

By far the largest rapid response found was that of clouds in the SW (a strong positive 'forcing' response of $0.94 \pm 0.43$ W m$^{-2}$), resulting from changes in cloud fraction alone. By way of comparison, Soden et al. (2008) diagnosed a mean cloud 'feedback' (in fact the net

response undifferentiated between forcing and warming responses) in CMIP3 coupled GCMs of 0.7 W $m^{-2}$ $K^{-1}$ (range 0–1.4 W $m^{-2}$ $K^{-1}$). This corresponds with a cloud change radiative perturbation of around 1.3 W $m^{-2}$ for a (model average) transient warming of $\sim$1.8 K at time of $CO_2$ doubling. Although, of course, the rapid response value found here is for a single model only, these figures suggest that it may form a very large component of the total cloud response (assuming the rapid forcing response under gradual $CO_2$ increase is similar in nature to that from a 'step' change).

A related point is that the relative importance of the rapid cloud response under transient climate change will depend upon the thermal inertia of the climate system, and the rate of change in forcing. For very large thermal inertia, or very rapid forcing increases, the 'rapid' cloud response (in the present model at least) will be dominant in defining total cloud radiative response. On the other hand, if thermal inertia is small (i.e. if global temperature response is fast), or if forcing were stabilised and the climate driven towards equilibrium then the balance would be expected to move closer to that found under equilibrium conditions (i.e. towards the right hand axis of Fig. 1).

A statistically equivalent cloud response was found between the two methods of analysis used here, and analysis of the vertical and latitudinal distribution of the contributions shows it to be related to cloud changes ranging from the tropical mid troposphere to the mid latitude lower troposphere, associated with decreased lower tropospheric RH in response to the $CO_2$ forcing. These regions also corresponded to regions of increased heating rates under $CO_2$ forcing, with consequent warming and decrease in RH (outside high latitude regions). Note that the role of changes in circulation on RH could be important and is not considered in the present study.

The pattern of SW $C_F$ response to the *SST forcing* was quite different to that from *$CO_2$ forcing*, with large positive radiation responses originating in the upper troposphere, low level tropical and subtropical negative contributions from increased cloud, and patterns of positive/negative contributions in mid latitude low levels associated with poleward migration of the storm tracks. SW $C_F$ feedback was diagnosed as positive ($0.36 \pm 0.09$ W $m^{-2}$ $K^{-1}$), but in addition there was a substantial negative SW $C_O$ feedback, producing an overall negative SW cloud feedback ($-0.42 \pm 0.20$ W $m^{-2}$ $K^{-1}$).

These findings suggest a complex picture in cloud response over different timescales, and from different processes. Clearly cloud fraction responses pose particular challenges in the SW—some low to mid tropospheric aspects, at least, respond rapidly to local $CO_2$ forcing, whilst other components, particularly in the upper troposphere are responding and 'feeding back' on the global temperature change. To a good approximation however, all other cloud components—viz LW cloud fraction changes, and both SW and LW cloud optical properties—(as well as water vapour, albedo and lapse rate responses) are behaving as classical 'feedbacks'. Note, however that these results apply to a single GCM only, and both Gregory and Webb (2008) and Andrews and Forster (2008) found significant CRF and clear sky differences between models. It would be of interest to investigate whether other GCMs are also responding in this way, particularly using PRP or a similar technique.

**Acknowledgments** The authors thank Leon Rotstayn, Carsten Frederiksen and two anonymous reviewers for their helpful comments. This work has been undertaken as part of the Australian Climate Change Science Program, funded jointly by the Department of Climate Change and Energy Efficiency, the Bureau of Meteorology and CSIRO.

## References

Andrews T, Forster PM (2008) $CO_2$ forcing induces semi-direct effects with consequences for climate feedback interpretations. Geophys Res Lett 35:L04802. doi:10.1029/2007GL032273

Bony S, Dufresne JL (2005) Marine boundary layer clouds at the heart of cloud feedback uncertainties in climate models. Geophys Res Lett 32(20):L20806

Bony S, Colman R, Kattsov V, Allan RP, Bretherton CS, Dufresne J-L, Hall A, Hallegatte S, Holland MM, Ingram W, Randall DA, Soden BJ, Tselioudis G, Webb MJ (2006) How well do we understand and evaluate climate change feedback processes? J Clim 19:3445–3482

Chou M, Suarez J, Ho C-H, Yan MM-H, Lee KT (1998) Parameterizations for cloud overlapping and shortwave single-scattering properties for use in general circulation and cloud ensemble models. J Clim 11:201–214

Colman RA (2003) A comparison of climate feedbacks in general circulation models. Clim Dyn 20:865–873

Colman RA (2004) On the structure of water vapour feedbacks in climate models. Geophys Res Lett 31:L21109. doi:10.1029/2004GL020708

Colman RA, Fraser JR, Rotstayn L (2001) Climate feedbacks in a general circulation model incorporating prognostic clouds. Clim Dyn 18:103–122

Gregory JM, Webb MJ (2008) Troposphere adjustment induces a cloud component in $CO_2$ forcing. J Clim 21:58–71

Gregory JM, Ingram WJ, Palmer MA, Jones GS, Stott PA, Thorpe RB, Lowe JA, Johns TC, Williams KD (2004) A new method for diagnosing radiative forcing and climate sensitivity. Geophys Res Lett 31:L03205

Hansen J, Sato M, Nazarenko L, Ruedy R, Lacis A, Koch D, Tegen I, Hall T, Shindell D, Santer B, Stone P, Novakov T, Homason L, Wang R, Wang Y, Jacob D, Hollandsworth-Frith S, Bishop L, Logan J, Thompson A, Stolarski R, Lean J, Willson R, Levitus S, Antonov J, Rayner N, Parker D, Christy J (2002) Climate forcings in Goddard Institute for Space Studies SI2000 simulations. J Geophys Res 107. doi:10.1029/2001JD001143

Hansen J, Sato M, Rudy R, Nazarenko L, Lacis A, Schmidt GA, Russel G, Aleinov I, Bauer M, Bauer S, Bell N, Cairns B, Canuto V, Chandler M, Cheng Y, Del Genio A, Faluvegi G, Fleming E, Friend A, Hall T, Jackman C, Kelley M, Kiang N, Koch D, Lean

J, Lerner J, Lo K, Menon S, Miller R, Romanou A, Shindell D, Stone P, Sun S, Tausnev N, Thresher D, Wielicki B, Wong T, Yao M, Zhang S (2005) Efficacy of climate forcings. J Geophys Res 110:D18104

Held IM, Soden BJ (2000) Water vapor feedback and global warming. Ann Rev Energy Environ 25:441–475

Lambert FH, Faull NE (2007) Tropospheric adjustment: the response of two general circulation models to a change in insolation. Geophys Res Lett 34:L03701

Randall DA, Wood RA, Bony S, Colman R, Fichefet T, Fyfe J, Kattsov V, Pitman A, Shukla J, Srinivasan J, Stouffer RJ, Sumi A, Taylor KE (2007) Climate models and their evaluation. In: Solomon S, Qin D, Manning M, Chen Z, Marquis M, Averyt KB, Tignor M, Miller HL (eds) Climate change 2007: the physical science basis. Contribution of working group i to the fourth assessment report of the intergovernmental panel on climate change. Cambridge University Press, Cambridge

Rotstayn LD (1997) A physically based scheme for the treatment of stratiform clouds and precipitation in large-scale models. 1: description and evaluation of the microphysical processes. Quart J R Meteorol Soc 123:1227–1282

Rotstayn LD, Ryan BF, Katzfey JJ (2000) A scheme for calculation of the liquid fraction in mixed-phase stratiform clouds in large-scale models. Mon Wea Rev 128:1070–1088

Shine KP, Cook J, Highwood EJ, Joshi MM (2003) An alternative to radiative forcing for estimating the relative importance of climate change mechanisms. Geophys Res Lett 30. doi:10.1029/2003GL018141

Soden BJ, Broccoli AJ, Hemler RS (2004) On the use of cloud forcing to estimate cloud feedback. J Clim 17:3661–3665

Soden BJ, Held IM, Colman RA, Shell KM, Kiehl JT, Shields CA (2008) Quantifying climate feedbacks using radiative kernels. J Clim 21:3504–3520

Stephens GL (2005) Cloud feedbacks in the climate system: a critical review. J Clim 18:237–273

Sun Z, Pethick D (2002) Comparison between observed and modelled radiative properties of stratocumulus clouds. Quart J R Meteorol Soc 128:2691–2712

Sun Z, Rikus LJ (1999) Improved application of exponential sum fitting transmissions to inhomogeneous atmosphere. J Geophy Res 104:6291–6303

Webb MJ, Senior CA, Sexton DMH, Ingram WJ, Williams KD, Ringer MA, McAvaney BJ, Colman RA, Soden BJ, Gudgel R, Knutson T, Emori S, Ogura T, Tsushima Y, Andronova N, Li B, Musat I, Bony S, Taylor KE (2006) On the contribution of local feedback mechanisms to the range of climate sensitivity in two GCM ensembles. Clim Dyn 27:17–38

Wetherald RT, Manabe S (1988) Cloud feedback processes in a GCM. J Atmos Sci 45:1397–1415